Rapid Communications

Direct and resonant breakup of radioactive ^{7}Be nuclei produced in the ^{112}Sn(^{6}Li, ^{7}Be) reaction

D. Chattopadhyay,[1,2] S. Santra,[1,3,*] A. Pal,[1] A. Kundu,[1,3] K. Ramachandran,[1] R. Tripathi,[3,4] T. N. Nag,[3,4] and S. Kailas[5]

[1]*Nuclear Physics Division, Bhabha Atomic Research Centre, Mumbai 400085, India*
[2]*Nuclear Physics Division, Saha Institute of Nuclear Physics, Kolkata 700064, India*
[3]*Homi Bhabha National Institute, Anushakti Nagar, Mumbai 400094, India*
[4]*RadioChemistry Division, Bhabha Atomic Research Centre, Mumbai 400085, India*
[5]*UM-CBS Centre for Excellence in Basic Sciences, Mumbai 400 098, India*

(Received 11 April 2020; accepted 1 July 2020; published 3 August 2020)

Cross sections for direct and resonant breakup of radioactive ^{7}Be nuclei produced in a transfer reaction ^{112}Sn(^{6}Li, ^{7}Be $\rightarrow \alpha + {}^{3}$He) ^{111}In have been measured. Breakup of ^{7}Be into α and ^{3}He cluster fragments via its resonant states of $7/2^{-}$(4.57 MeV) and $5/2^{-}$ (6.73 MeV) in the continuum have been identified for the first time using the measured distribution of α-^{3}He relative energy and the reaction Q value obtained from the α-^{3}He coincident events. The breakup cross sections extracted from the efficiency corrected coincidence yield compares well with the results of the coupled-channels calculations. Significant cross sections for breakup of ^{7}Be into its cluster fragments directly or through resonant states highlight the importance of the ground-state structure of ^{7}Be as a cluster of α and ^{3}He.

DOI: 10.1103/PhysRevC.102.021601

The study of nuclear reactions using weakly bound stable and radioactive ion beams is a topic of great interest. Most of the radioactive light nuclei are weakly bound and exhibit cluster structure in their ground states (g.s.). Being weakly bound, these projectile nuclei are prone to breakup into two or more cluster fragments during the interaction with a target nucleus. The presence of additional breakup channels in the above reactions compared to the ones involving strongly bound projectiles leads to several interesting observations on the outgoing channels, especially at beam energies around the Coulomb barrier. Such observations include: (i) suppression or enhancement of complete fusion cross sections [1,2], (ii) enhancement in the inclusive α-particle production [3–5], (iii) breakup threshold anomaly in the energy dependence of the optical model potentials obtained from elastic-scattering angular distributions [6,7], and (iv) enhancement in the peak-to-valley ratio of the fission fragment mass distribution as well as in the width of the folding angle distribution [8,9]. The breakup of the projectile may occur in two modes: direct or sequential. In the second mode, one of the possibilities is the transition of the projectile nucleus to any of its excited states in the continuum with finite lifetimes (resonant states) followed by its breakup into two cluster fragments. The search for these breakup channels through different resonance states of the weakly bound stable or unstable nuclei is of current interest.

In recent years, several studies have been carried out using weakly bound stable nuclei ^{6,7}Li and ^{9}Be to understand the role of different breakup channels on elastic-scattering, fusion, and fission reactions at near-barrier energies and their consequences on high yield of inclusive α production [1–7,10–19]. In addition to the direct and resonant breakup channels, the cross sections of the individual transfer-induced breakup channels play an important role in providing correct coupling strength needed for realistic coupled-channels calculations to find their effects on elastic as well as fusion cross sections. For reactions involving weakly bound unstable nuclei with medium and heavy mass targets, a large enhancement of total reaction cross sections has been observed [20]. There have been several studies focused towards finding the probable reaction channels which are mainly responsible for such an enhancement. The properties of these nuclei also influence the results of explosive astrophysical events, such as supernovas. However, direct measurement of structural properties of these nuclei is very challenging because of their short lifetimes and limited availability. So, one should search for indirect methods to get the structural data of these rare exotic nuclei. One of the possibilities is to produce these radioactive nuclei by transfer reactions involving weakly bound stable nuclei and then study their breakup reaction mechanisms. For example, the radioactive ^{7}Be nuclei can be produced by a $1p$-pickup reaction involving the weakly bound stable projectiles of ^{6}Li, i.e., (^{6}Li, ^{7}Be) reaction. ^{7}Be lies on the proton-rich side of the line of stability, and it is weakly bound with a threshold energy of 1.59 MeV for its breakup into ^{3}He and α. So, if ^{7}Be is formed by the above transfer reaction with excitation energy above its breakup threshold, then, it will breakup into two fragments: ^{3}He and α. The study of breakup mechanisms in the reactions involving ^{7}Be as a projectile is very important for understanding the cluster structure of ^{7}Be. This structural information can be used as the input to the study of proton halo nucleus ^{8}B (of which ^{7}Be is considered to be the core), thus, adding further importance to the study of ^{7}Be breakup.

*ssantra@barc.gov.in

The effect of breakup of $^{7}\mathrm{Be} \rightarrow {}^{3}\mathrm{He} + \alpha$ on elastic-scattering angular distribution has been studied in Refs. [21–23] at energies near the Coulomb barrier. In the energy dependence behavior of the optical potentials obtained from the elastic-scattering analysis, a usual threshold anomaly has been observed indicating no significant effect of breakup. However, the studies in Refs. [23,24] show significant effect of breakup of ^{7}Be on elastic scattering where the importance of both direct as well as resonant breakup has been pointed out.

Attempts have been made to measure the cross sections for breakup of $^{7}\mathrm{Be} \rightarrow \alpha + {}^{3}\mathrm{He}$ in reactions $^{7}\mathrm{Be} + {}^{12}\mathrm{C}$ [25] and ^{58}Ni [26]. An unambiguous measurement of noncapture breakup cross sections is possible only by detecting both ^{3}He and α in coincidence. In the study of $^{7}\mathrm{Be} + {}^{12}\mathrm{C}$ by Amro *et al.* [25], no significant ^{3}He-α coincidence counts have been observed. The production of the majority of ^{3}He and α particles in direct reactions could be explained in terms of α and ^{3}He cluster transfers, respectively, on the basis of experimentally observed forward peaked angular distributions and the results of coupled-channels calculations. In a study on the measurement of the coincidence of fission fragments with light charged particles, such as α or ^{3}He in the $^{7}\mathrm{Be} + {}^{238}\mathrm{U}$ reaction, Raabe *et al.* [27] also emphasize on the dominance of cluster transfer mechanism. Mazzocco *et al.* [26] have made a detailed study on both experimental and theoretical cross sections for breakup of ^{7}Be in the $^{7}\mathrm{Be} + {}^{58}\mathrm{Ni}$ reaction at $E_{\mathrm{lab}} = 21.5$ MeV. Results of coupled-channels calculations predicted a significant breakup cross section ($\approx$10.8 mb) in contrast to their experimental observation [26]. The limited geometrical efficiencies of the detectors used for the above measurements appear to have resulted in the observation of only a few ^{3}He-α coincidence counts corresponding to the breakup of ^{7}Be. Although, an estimated upper limit on the breakup cross section has been found to corroborate with the results of coupled-channels calculations. There is no experimental data available in the literature on the cross section for ^{7}Be breakup obtained directly from the measured ^{3}He-α coincidence counts. The observed differences between theoretical prediction and different measurements warrants further experimental and theoretical investigations on the cross sections for breakup of ^{7}Be into $^{3}\mathrm{He} + \alpha$. One of the reasons for such low ^{3}He-α coincidence counts measured in Ref. [26] for $^{7}\mathrm{Be} + {}^{58}\mathrm{Ni}$ could be due to the missing events corresponding to the resonant breakup of ^{7}Be. There are two known resonance states of ^{7}Be at 4.57 MeV ($7/2^{-}$) and 6.73 MeV ($5/2^{-}$) [28] to which ^{7}Be is expected to be excited with a good probability followed by a breakup into $^{3}\mathrm{He} + \alpha$.

The experimental cross section for both direct as well as resonant breakup of ^{7}Be is of utmost importance in order not only to understand the complete breakup reaction mechanism, but also to derive the astrophysical S factor for the capture reaction $^{3}\mathrm{He} + \alpha \rightarrow {}^{7}\mathrm{Be}$. With the above motivation, a detailed study of breakup reactions involving both direct and sequential breakup of the radioactive nuclei ^{7}Be produced in $^{112}\mathrm{Sn}(^{6}\mathrm{Li}, {}^{7}\mathrm{Be})$ reaction has been taken up in the present Rapid Communication using a big Si-strip detector array covering a large solid angle with good granularity and energy resolution.

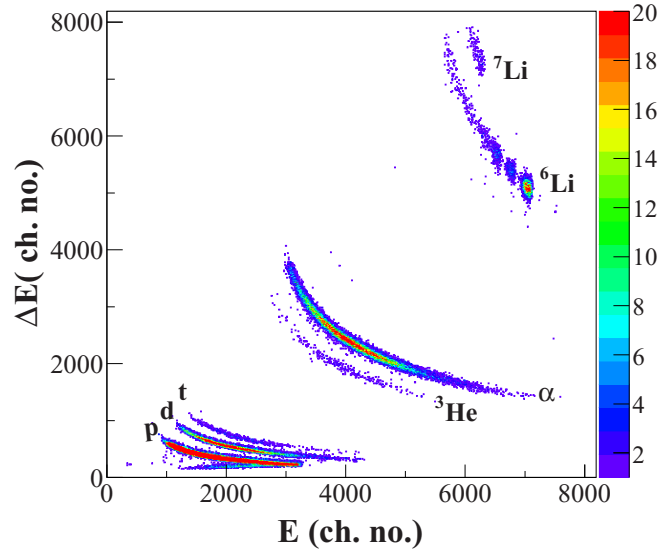

FIG. 1. A typical two-dimensional (ΔE versus E) raw spectrum obtained from one of the vertical strips at 95° and $E_{\mathrm{beam}} = 30$ MeV, clearly identifying different particle bands with $Z = 1$–3.

This Rapid Communication reports the results of experimental breakup cross section of ^{7}Be into $^{3}\mathrm{He} + \alpha$ via its direct as well as resonance modes. Coupled reaction channels (CRC) calculations have been performed to understand the measured cross sections. Experimental and/or theoretical cross sections have been compared to find out the contributions of the breakup channels to inclusive α production and understand the underlying reaction mechanism.

Exclusive measurements have been carried out for the $^{6}\mathrm{Li} + {}^{112}\mathrm{Sn}$ reaction at a beam energy of 30 MeV using the 14-UD Pelletron-LINAC Accelerator facility in Mumbai. Self-supporting enriched ($\approx$99.5%) ^{112}Sn foil having a thickness of $\approx$540 μg/cm^{2} was used as a target. Five telescopes (S1–S5) of double-sided Si strip detectors covering a total angular range of $\approx$93° were placed on one of the two rotatable arms inside a 1.5-m diameter scattering chamber to detect the breakup fragments. The cone angles that need to be covered to detect the breakup proceeding through the above resonance states are $\approx$40° and 53°, respectively. Two Si-surface barrier detectors (of thicknesses $\approx$1000 μm) kept at $\pm$20° were used to monitor incident flux by measuring the Rutherford scattering. In addition, there were five telescopes (T1–T5) of single surface barrier detectors (with $\Delta E \approx 50$, $E \approx$ 1000–2000 μm) placed on the second arm of the scattering chamber to measure the elastic-scattering cross sections in additional angles, particularly, the forward ones. A typical two-dimensional spectrum of ΔE versus E is shown in Fig. 1 where the two bands corresponding to ^{3}He and α particles are clearly separated.

In this Rapid Communication, we focus on (^{6}Li, ^{7}Be), i.e., the 1p-pickup reaction followed by breakup into $\alpha + {}^{3}$He particles. The coincidence yields in any two pixels with α particles in one pixel and the ^{3}He particle in any other pixel of another strip have been extracted independently by putting two-dimensional gates on, respective, particle bands of the

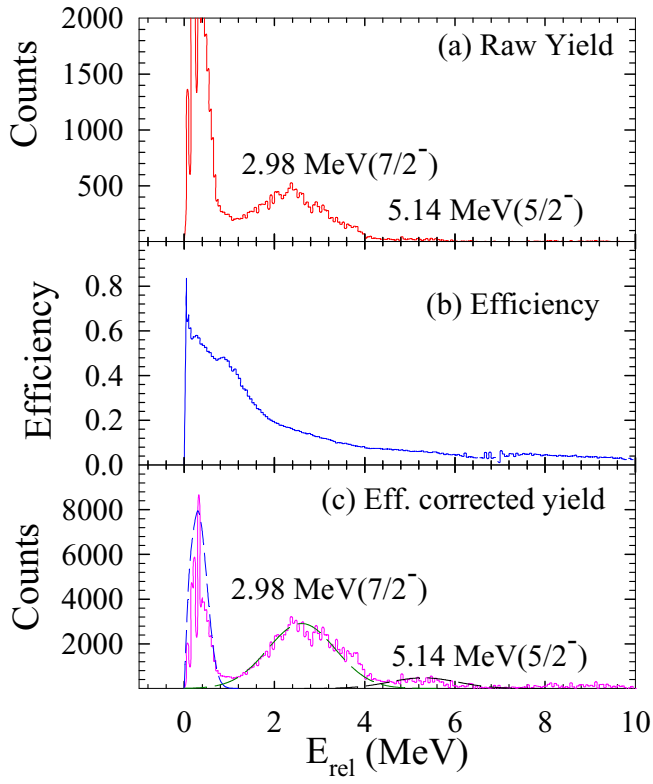

FIG. 2. (a) Distribution of relative energy $E_{\rm rel}$ of the coincident α-^{3}He breakup fragments without efficiency correction, (b) the efficiency of the detector array as a function of relative energy, and (c) the efficiency corrected $E_{\rm rel}$ distribution.

spectra obtained from the strip telescopes. The relative energy distribution between two breakup fragments infer about the excitation energy of the projectilelike nuclei above their breakup threshold through which the breakup occurs. The relative energy "$E_{\rm rel}$" of two breakup fragments [30] ^{3}He and α was reconstructed using the measured energies and emission angles. The expression of relative energy for the α-^{3}He pair is given by

$$E_{\rm rel} = \frac{m_1E_2 + m_2E_1 - 2\sqrt{m_1m_2E_1E_2}\cos\,\theta_{12}}{m_1 + m_2}. \qquad (1)$$

From the relative energy distribution without efficiency correction as shown in Fig. 2(a), it is observed that the breakup yield of ^{7}Be $\rightarrow \alpha + {}^3$He is peaking around 2.98 MeV and 5.14 MeV corresponding to $7/2^-$ and $5/2^-$ states of ^{7}Be, respectively. To confirm that these peaks genuinely represent the resonant states of ^{7}Be, a Monte Carlo simulation was carried out to obtain the relative energy-dependent efficiency. The breakup fragments were assumed to be emitted isotropically in the rest frame of the outgoing projectilelike nucleus ^{7}Be before it broke up. The $E_{\rm rel}$ and efficiency of the detector have been determined event by event. This efficiency distribution was applied to the raw data to obtain the efficiency corrected $E_{\rm rel}$ distribution.

For ^{7}Be breaking into α and ^{3}He, the $E_{\rm rel}$ distribution without efficiency correction, the $E_{\rm rel}$-dependent efficiency of the detector array, and the $E_{\rm rel}$ distribution with efficiency correction have been shown in Figs. 2(a)–2(c), respectively. It is interesting to see from the Fig. 2(c), similar to Fig. 2(a), that, apart from the direct breakup at low energy, there are two dominant peaks at 2.98 and 5.14 MeV which correspond to the first and second resonance states of $7/2^-$ (4.57 MeV) and $5/2^-$ (6.73 MeV), respectively (see Table I). The width of the $7/2^-$ state is found to be much larger than the value available in the literature. This broadening could be due to the differential postbreakup Coulomb acceleration of ^{3}He and ^{4}He fragments along with the effect of the fragment orientations. It may be emphasized that the breakup of ^{7}Be into ^{3}He + α through its two resonant states is observed for the first time in the present Rapid Communication.

To find out the excitations of the residual target nuclei associated with the breakup process, the Q-value distribution of each of the breakup events of ^{7}Be $\rightarrow \alpha + {}^3$He has been generated from the following relation [14]:

$$Q = E_\alpha + E_{^3\rm He} + E_{\rm loss} + E_{\rm recoil} - E_{\rm beam}, \qquad (2)$$

where E_α and $E_{^3\rm He}$ are the laboratory energies of the breakup fragments α and ^{3}He, $E_{\rm beam}$ is the beam energy, $E_{\rm loss}$ is the energy loss in the target calculated at half-thickness, and $E_{\rm recoil}$ is the recoil energy of the residual target nucleus in the laboratory frame. The Q-value distributions of the corresponding reactions have been shown in Fig. 3. Two-dimensional plots of $E_{\rm rel}$ versus the Q value can reveal the information about the excitations of targetlike fragment associated with the particular breakup mode of the projectilelike fragment. From Fig. 4, it can be concluded that the breakup is mainly occurring via the g.s. of the target nuclei ($Q_{gg} = -3.55$ MeV). In addition, there are events with Q values smaller than -3.55 MeV that correspond to the breakup events accompanied by many low-lying excitations (up to $\approx$1.2 MeV) of the residual nucleus ^{111}In.

Differential cross sections for ^{7}Be $\rightarrow \alpha + {}^3$He breakup channels have been obtained following the same procedure as adopted in Refs. [11,12]. Using reconstructed events for $\alpha + {}^3$He breakup, a distribution of events corresponding to different θ, ϕ's of the outgoing ^{7}Be* just before breakup,

TABLE I. Energies and widths of the resonance peaks observed in relative energy distribution compared with the literature values [29].

	Present Rapid Communication		Literature	
State	$E_{\rm rel}$ (MeV)	Γ (MeV)	$E_{\rm rel}$ (MeV)	Γ (MeV)
^{7}Be ($7/2^-$)	2.60	1.76	2.98	0.175
^{7}Be ($5/2^-$)	5.30	1.76	5.14	1.20

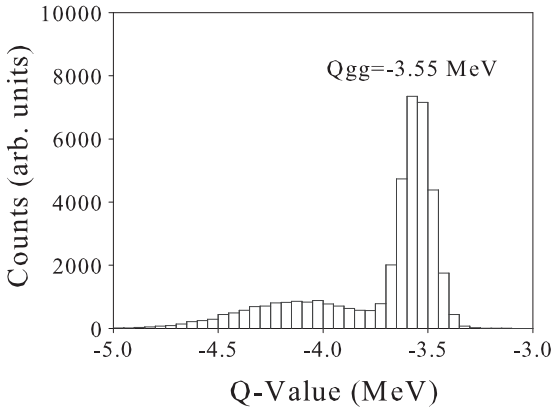

FIG. 3. Q-value distribution of the reaction ^{112}Sn(^{6}Li, ^{7}Be $\rightarrow \alpha + {}^{3}$He) ^{111}In at $E_{\rm beam} = 30$ MeV.

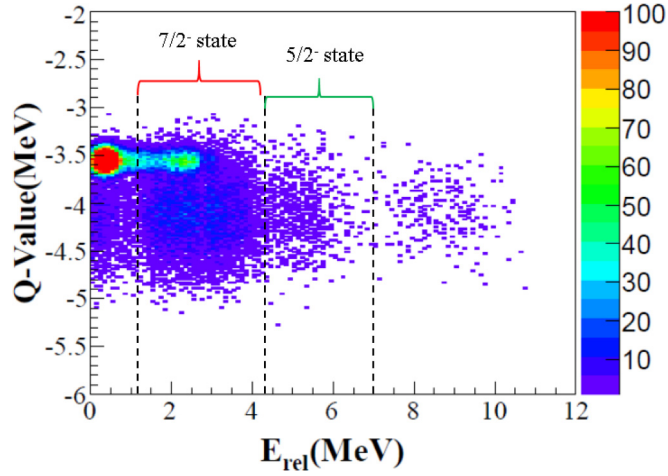

FIG. 4. Two-dimensional plot of $E_{\rm rel}$ versus the Q value showing the distribution of events with different projectilelike and targetlike excitations for the $\alpha + {}^{3}$He breakup.

was generated. Now, for each $\theta(^{7}\text{Be}^{*})$ bin, the efficiency corrected relative energy distribution $[Y_i^{\rm eff}(\theta) = Y_i^{\rm raw}(\theta)/\zeta_i]$ was obtained by summing over all $\phi(^{7}\text{Be}^{*})$ coverage of a detector array corresponding to the same $\theta(^{7}\text{Be}^{*})$ bin. Here, $Y_i^{\rm raw}(\theta)$ represents the yield of the "i"th bin of the relative energy between ϵ_i and $\epsilon_i + d\epsilon$ without the efficiency correction, and ζ_i is the efficiency of the detector array for the same relative energy bin. For a particular θ bin, the coincidence yields under the peaks corresponding to the resonances of $7/2^{-}$($E_{\rm rel}$ = 1.2–4.3 MeV) and $5/2^{-}$($E_{\rm rel}$ = 4.3–7.0 MeV) in the relative energy distribution have been extracted individually by integrating $Y_i^{\rm eff}(\theta)$ in steps of $d\epsilon$ (=0.05 MeV) over the respective $E_{\rm rel}$ range ($\Delta\epsilon = N\, d\epsilon$).

Differential breakup cross section for each of the resonance states is extracted from the following relation:

$$\frac{d\sigma^{br}}{d\Omega}(\theta) = \frac{\sum_{i=1}^{N} Y_i^{\rm eff}(\theta)}{Y_{\rm el}(\theta)} \frac{d\sigma^{\rm el}}{d\Omega}(\theta), \tag{3}$$

where $Y_{\rm el}(\theta)$ is the yield of elastic scattering in the solid angle corresponding to the element $\Delta\theta(^{7}\text{Be}^{*})$, $\Delta\phi(^{7}\text{Be}^{*})$, and $\frac{d\sigma^{\rm el}}{d\Omega}(\theta)$ is the differential elastic-scattering cross section. The latter was obtained by normalizing: (i) $Y_{\rm el}(\theta)$ to the monitor yield $Y_m(\theta_m)$ corresponding to Rutherford scattering and (ii) their solid angles. Thus, differential cross sections for the direct breakup of ^{7}Be $\rightarrow \alpha + {}^{3}$He with relative energy in the range of 0–1.2 MeV have been deduced and shown as hollow circles in Fig. 5(a). Similarly, the cross sections obtained for ^{7}Be $\rightarrow \alpha + {}^{3}$He breakup via $7/2^{-}$ and $5/2^{-}$ resonances are shown as hollow circles in Figs. 5(b) and 5(c), respectively. Although there are evidences for direct breakup mode as observed in the measurements of Refs. [25,26], the cross sections for the direct breakup as well as the resonant breakup modes via the states of $7/2^{-}$ and $5/2^{-}$ are observed in the present Rapid Communication for the first time.

The $1p$ pickup followed by breakup into $\alpha + {}^{3}$He, i.e., (^{6}Li, ^{7}Be $\rightarrow \alpha + {}^{3}$He) reaction is found to be one of the important breakup channels and, thus, responsible for α-particle production in outgoing channels of the ^{6}Li + ^{112}Sn reaction system. The present section focuses on the theoretical understanding of the experimentally measured cross sections of direct and resonant breakup channels of radioactive nuclei of ^{7}Be which is produced in $1p$-pickup reaction. When ^{7}Be is formed with excitation energy above its breakup threshold (1.586 MeV), it breaks into an α-^{3}He pair. Hence, the cross section for the $1p$-pickup reaction leading to the formation of ^{7}Be with excitation energy above 1.586 MeV is considered to be equal to the breakup cross section of ^{7}Be into $\alpha + {}^{3}$He. CRC calculations using the nuclear reaction code FRESCO [31] have been performed to estimate the $1p$-pick up cross section. For the channels that are coupled in the calculations, only two mass partitions with outgoing channels ^{6}Li + ^{112}Sn (for

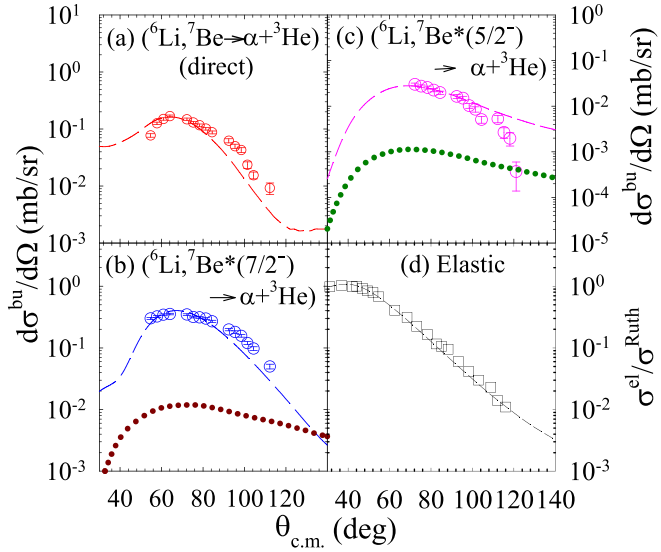

FIG. 5. Cross sections for direct and sequential breakup of ^{7}Be $\rightarrow \alpha + {}^{3}$He for its $7/2^{-}$ and $5/2^{-}$ resonances [(a)–(c), respectively] and elastic scattering (d). The results of the coupled-channels calculations using FRESCO are shown by dashed and dotted lines considering ^{7}Be continuum states as ^{6}Li$(0^{+}) + p$ and ^{6}Li$(1^{+}) + p$, respectively.

TABLE II. Structure information and spectroscopic amplitudes (SAs) for the overlaps $A = C + x$ corresponding to different states of the nuclei A, C, and x used in the CRC calculations for the (^{6}Li, ^{7}Be) reaction.

Nucleus (A)	C	x	BE (MeV)	$nlj(x)$	SA
^{7}Be($7/2^-$)	^{6}Li(0^+)	p	4.6990	$1f_{7/2}$	1.000
^{7}Be($5/2^-$)	^{6}Li(0^+)	p	2.4390	$1f_{5/2}$	0.572
^{112}Sn(0^+)	^{111}In (g.s., $9/2^+$)	p	7.5541	$1g_{9/2}$	1.000
^{112}Sn(0^+)	^{111}In (0.537 MeV, $1/2^-$)	p	7.0181	$2p_{1/2}$	0.680
^{112}Sn(0^+)	^{111}In (0.803 MeV, $3/2^-$)	p	6.7521	$2p_{3/2}$	0.680
^{112}Sn(0^+)	^{111}In (1.101 MeV, $5/2^+$)	p	6.5371	$2d_{5/2}$	0.680

elastic and inelastic scatterings) and ^{7}Be + ^{111}In (for the $+1p$ transfer) have been considered. In the first mass partition, ^{6}Li has been considered to be in ground state as well as in the 0^+ excited state, and ^{112}Sn has been considered to be in the ground state. In the second mass partition corresponding to $1p$ pickup, i.e., the (^{6}Li, ^{7}Be) reaction, the outgoing channels included in the couplings correspond to: (i) 15 nonresonant states of ^{7}Be (five each with relative angular momentum of $L = 0$–2) up to an excitation energy of 1.2 MeV, (ii) two resonant states ($7/2^-$ and $5/2^-$) of ^{7}Be, and (iii) the ground-state ($9/2^+$) plus three excited states of ^{111}In. It is assumed that ^{7}Be in its resonant states is formed as ^{6}Li(0^+) + p [28] via the $+1p$-transfer reaction. The details of the states (n, l, s, j) coupled and the spectroscopic amplitudes for the overlaps $\langle ^7\text{Be} \,|\, ^6\text{Li}(0^+) + p\rangle$ and $\langle ^{112}\text{Sn} \,|\, ^{111}\text{In} + p\rangle$ used in the CRC calculations for the resonance states of ^{7}Be and the target states are given in Table II. The values of spectroscopic amplitudes required for the present calculations are not available in the literature. So, new values of spectroscopic amplitudes are assigned to the states coupled to reproduce the observed cross sections. For nonresonant states up to excitation energy of 1.2 MeV above breakup threshold, each energy bin (in steps of 0.4 MeV) with every possible spin-parity corresponding to $L = 0$–2 is taken as an independent channel. The same value of spectroscopic amplitude (SA = 0.26) has been assumed for all these channels to reproduce the measured direct breakup cross section.

The real and imaginary potentials of the Woods-Saxon volume form with $V_0 = 17.85$ MeV, $r_0 = 1.255$ fm, $a_0 = 0.700$ fm, $W_0 = 19.47$ MeV, $r_w = 1.265$ fm, and $a_w = 0.750$ fm, obtained from the optical model fit to the measured elastic-scattering angular distribution have been used for the elastic-inelastic mass partition. For the transfer mass partition, the real part of the optical potential was the same as that of the entrance channel mass partition, but the imaginary part was taken to be of short-range Woods-Saxon square form with $W_0 = 10.00$ MeV, $r_w = 1.10$ fm and $a_w = 0.4$ fm. The binding potentials for $p + ^6$Li are taken to be real and also of Woods-Saxon volume form with $V_0 = 30.0$ MeV, $r_0 = 1.20$ fm, $a_0 = 0.60$ fm, $V_{so} = 6.20$ MeV, $r_{so} = 1.18$ fm, and $a_{so} = 0.720$ fm where the subscript "so" corresponds to the spin-orbit term. The depth is automatically varied to reproduce the binding energy. Similarly, the binding potential parameters used for $p + ^{111}$In are $V_0 = 30.0$ MeV, $r_0 = 1.20$ fm, $a_0 = 0.60$ fm, $V_{so} = 6.20$ MeV, $r_{so} = 1.18$ fm, and $a_{so} = 0.72$ fm. The FRESCO calculations, represented by dashed lines in Fig. 5, reproduce the experimental data reasonably well. The dotted lines represent calculations assuming ^{7}Be as ^{6}Li(1^+) + p which underestimate the experimental data suggesting the importance of the consideration of ^{7}Be continuum states as ^{6}Li(0^+) + p.

To understand the overall reaction mechanism of breakup of ^{6}Li in the field of target nucleus ^{112}Sn at $E_{beam} = 30$ MeV, a comprehensive list of experimental and theoretical cross sections for different breakup channels obtained from the present Rapid Communication along with the data available in the literature [3] has been compiled in Table III. The cross sections for inclusive breakup α (given in the table) are found to be much larger than all the known noncapture breakup channels combined together that make up only ≈15%. It indicates the existence of other possible sources of α production, such as incomplete fusion (where one of the breakup fragments which is complementary to α is captured by the target) and new noncapture breakup modes that need further investigations.

To summarize, exclusive measurements for both direct and resonant breakup modes of radioactive nuclei of ^{7}Be have been carried out. The cross sections for breakup of ^{7}Be into $\alpha + ^3$He through its first ($7/2^-$) and second ($5/2^-$) resonance

TABLE III. Experimental and theoretical cross sections for different breakup channels of ^{6}Li in the field of target nucleus ^{112}Sn at $E_{beam} = 30$ MeV.

Reaction channel	σ^{expt} (mb)	σ^{theory} (mb)	Reference
$^6\text{Li}^* \rightarrow \alpha + d$ (resonant)	34.0 ± 4.0	34.6	[3]
$^6\text{Li}^* \rightarrow \alpha + d$ (direct)	12.0 ± 2.0	12.0	[3]
$^6\text{Li} \rightarrow ^5\text{Li}^* \rightarrow \alpha + p$	28.1 ± 4.0	19.2	[3]
$^6\text{Li} \rightarrow ^8\text{Be}^* \rightarrow \alpha + \alpha$	4.2 ± 0.8	4.79	[3]
$^6\text{Li} \rightarrow ^7\text{Be}^* \rightarrow \alpha + ^3\text{He}$ (direct)	0.63 ± 0.06	0.64	Present Rapid Communication
$^6\text{Li} \rightarrow ^7\text{Be}^* \rightarrow \alpha + ^3\text{He}$ (first resonance state)	1.58 ± 0.10	1.55	Present Rapid Communication
$^6\text{Li} \rightarrow ^7\text{Be}^* \rightarrow \alpha + ^3\text{He}$ (second resonant state)	0.09 ± 0.01	0.09	Present Rapid Communiication
Inclusive breakup α	592 ± 35		[3]

states along with the direct breakup mode have been measured for the first time. Coupled-channels calculations explain the measured data reasonably well. The experimental and theoretical results on direct and resonant breakup of ^{7}Be presented here provide information on new breakup modes leading to an improved understanding of projectile breakup mechanism. The inclusive α-particle production cross section is found to be much larger compared to the combined cross sections of all the known noncapture breakup channels with α as one of the outgoing particles, indicating the existence of other possible sources of α production, such as incomplete fusion and new breakup modes. Measurements of present noncapture breakup channels opens up the possibilities of finding new breakup modes contributing to the total cross sections for noncapture breakup, be it resonant or nonresonant.

S.S. and D.C. acknowledge the financial support of BRNS through the DAE-SRC Project No. "2012/21/11-BRNS/1090." S.K. acknowledges INSA (Indian National Science Academy) for the award of Senior Scientist fellowship.

[1] P. R. S. Gomes, D. R. Otomar, T. Correa, L. F. Canto, J. Lubian, R. Linares, D. H. Luong, M. Dasgupta, D. J. Hinde, and M. H. Hussein, J. Phys. G: Nucl. Part. Phys. **39**, 115103 (2012).

[2] P. K. Rath, S. Santra, N. L. Singh, B. K. Nayak, K. Mahata, R. Palit, K. Ramachandran, S. K. Pandit, A. Parihari, A. Pal *et al.*, Phys. Rev. C **88**, 044617 (2013).

[3] D. Chattopadhyay, S. Santra, A. Pal, A. Kundu, K. Ramachandran, R. Tripathi, D. Sarkar, S. Sodaye, B. K. Nayak, A. Saxena *et al.*, Phys. Rev. C **94**, 061602(R) (2016).

[4] S. Santra, S. Kailas, V. V. Parkar, K. Ramachandran, V. Jha, A. Chatterjee, P. K. Rath, and A. Parihari, Phys. Rev. C **85**, 014612 (2012).

[5] S. K. Pandit, A. Shrivastava, K. Mahata, V. V. Parkar, R. Palit, N. Keeley, P. C. Rout, A. Kumar, K. Ramachandran, S. Bhattacharyya *et al.*, Phys. Rev. C **96**, 044616 (2017).

[6] M. S. Hussein, P. R. S. Gomes, J. Lubian, and L. C. Chamon, Phys. Rev. C **73**, 044610 (2006).

[7] S. Santra, S. Kailas, K. Ramachandran, V. V. Parkar, V. Jha, B. J. Roy, and P. Shukla, Phys. Rev. C **83**, 034616 (2011).

[8] I. Itkis *et al.*, Phys. Lett. B **640**, 23 (2006).

[9] S. Santra, A. Pal, P. K. Rath, B. K. Nayak, N. L. Singh, D. Chattopadhyay, B. R. Behera, V. Singh, A. Jhingan, P. Sugathan *et al.*, Phys. Rev. C **90**, 064620 (2014).

[10] S. Santra, V. V. Parkar, K. Ramachandran, U. K. Pal, A. Shivastava, B. J. Roy, B. K. Nayak, A. Chatterjee, R. K. Choudhury, and S. Kailas, Phys. Lett. B **677**, 139 (2009).

[11] D. Chattopadhyay, S. Santra, A. Pal, A. Kundu, K. Ramachandran, R. Tripathi, B. J. Roy, T. N. Nag, Y. Sawant, B. K. Nayak *et al.*, Phys. Rev. C **97**, 051601(R) (2018).

[12] D. Chattopadhyay, S. Santra, A. Pal, A. Kundu, K. Ramachandran, R. Tripathi, B. J. Roy, Y. Sawant, B. K. Nayak, A. Saxena *et al.*, Phys. Rev. C **98**, 014609 (2018).

[13] S. K. Pandit, A. Shrivastava, K. Mahata, N. Keeley, V. V. Parkar, P. C. Rout, K. Ramachandran, I. Martel, C. S. Palshetkar, A. Kumar *et al.*, Phys. Rev. C **93**, 061602(R) (2016).

[14] D. H. Luong, M. Dasgupta, D. J. Hinde, R. du Rietz, R. Rafiei, C. J. Lin, M. Evers, and A. Diaz-Torres, Phys. Rev. C **88**, 034609 (2013).

[15] A. Shrivastava, A. Navin, N. Keeley, K. Mahata, K. Ramachandran, V. Nanal, V. Parkar, A. Chatterjee, and S. Kailas, Phys. Lett. B **633**, 463 (2006).

[16] S. Santra, V. V. Parkar, K. Ramachandran, A. Shrivastava, B. J. Roy, B. K. Nayak, A. Chatterjee, R. K. Choudhury, and S. Kailas, Nucl. Phys. A **834**, 186c (2010).

[17] A. Pal, S. Santra, D. Chattopadhyay, A. Kundu, K. Ramachandran, R. Tripathi, B. J. Roy, T. N. Nag, Y. Sawant, D. Sarkar *et al.*, Phys. Rev. C **96**, 024603 (2017).

[18] A. Pal, S. Santra, D. Chattopadhyay, A. Kundu, A. Jhingan, P. Sugathan, N. Saneesh, M. Kumar, N. L. Singh, A. Yadav *et al.*, Phys. Rev. C **98**, 031601(R) (2018).

[19] A. Pal, S. Santra, D. Chattopadhyay, A. Kundu, A. Jhingan, P. Sugathan, B. K. Nayak, A. Saxena, and S. Kailas, Phys. Rev. C **99**, 024620 (2019).

[20] I. Tanihata *et al.*, Prog. Part. Nucl. Phys. **68**, 215 (2013).

[21] K. C. C. Pires *et al.*, in *Proceedings of the 12th InternationalConference on Nuclear Reaction Mechanisms, Varenna, Italy, 2009*, edited by F. Cerutti and A. Ferrari, Vol. 2 (CERN, Geneva, 2010), p. 337.

[22] J. C. Zamora, V. Guimaraes, A. Barioni, A. Lepine-Szily, R. Lichtenthaler, P. N. de Faria, D. R. Mendes, Jr., L. R. Gasques, J. M. B. Shorto *et al.*, Phys. Rev. C **84**, 034611 (2011).

[23] G. Tabacaru, A. Azhari, J. Brinkley, V. Burjan, F. Carstoiu, C. Fu, C. A. Gagliardi, V. Kroha, A. M. Mukhamedzhanov, X. Tang *et al.*, Phys. Rev. C **73**, 025808 (2006).

[24] K. Horii, M. Takashina, T. Furumoto, Y. Sakuragi, and H. Toki, Phys. Rev. C **81**, 061602(R) (2010).

[25] H. Amro, F. D. Becchetti, Yu Chen, H. Jiang, M. Ojaruega, M. J. Golobish, H. C. Griffin, J. J. Kolata, B. Skorodumov, G. Peaslee *et al.*, Eur. Phys. J. Special Topics **150**, 1 (2007).

[26] M. Mazzocco, D. Torresi, D. Pierroutsakou, N. Keeley, L. Acosta, A. Boiano, C. Boiano, T. Glodariu, A. Guglielmetti, M. LaCommara *et al.*, Phys. Rev. C **92**, 024615 (2015).

[27] R. Raabe, C. Angulo, J. L. Charvet, C. Jouanne, L. Nalpas, P. Figuera, D. Pierroutsakou, M. Romoli, and J. L. Sida, Phys. Rev. C **74**, 044606 (2006).

[28] K. Arai, D. Baye, and P. Descouvemon, Nucl. Phys. A **699**, 963 (2002).

[29] D. R. Tilley, C. M. Cheves, J. L. Godwin, G. M. Hale, H. M. Hofmann, J. H. Kelley, C. G. Sheu, and H. R. Weller, Nucl. Phys. A **708**, 3 (2002).

[30] R. J. de Meijer, and R. Kamermans, Rev. Mod. Phys. **57**, 147 (1985).

[31] I. J. Thompson, Comput. Phys. Rep. **7**, 167 (1988)